scientific reports

Check for updates

OPEN

Phenotypic variability of *RP1*-related inherited retinal dystrophy associated with the c.5797 C > T (p.Arg1933*) variant in the Japanese population

Keigo Natsume, Taro Kominami✉, Kensuke Goto, Yoshito Koyanagi, Taiga Inooka, Junya Ota, Kenichi Kawano, Kazuhisa Yamada, Daishi Okuda, Kenya Yuki, Koji M. Nishiguchi & Hiroaki Ushida

The phenotypes of *RP1*-related inherited retinal dystrophies (*RP1*-IRD), causing autosomal dominant (AD) and autosomal recessive (AR) diseases, vary depending on specific *RP1* variants. A common nonsense mutation near the C-terminus, c.5797 C > T (p.Arg1933*), is associated with *RP1*-IRD, but the exact role of this mutation in genotype-phenotype correlation remains unclear. In this study, we retrospectively analyzed patients with *RP1*-IRD (*N* = 42) from a single center in Japan. AR *RP1*-IRD patients with the c.5797 C > T mutation (*N* = 14) mostly displayed macular dystrophy but rarely retinitis pigmentosa or cone-rod dystrophy. Conversely, AR *RP1*-IRD patients without the c.5797 C > T mutation, including those with other pathogenic *RP1* variants, were mostly diagnosed with severe retinitis pigmentosa. Full-field electroretinograms were significantly better in patients homozygous or compound heterozygous for the c.5797 C > T mutation than in those without this mutation, corresponding to their milder phenotypes. Clinical tests also revealed a slower onset of age and a better mean deviation value with the static visual field in AR *RP1*-IRD patients with the c.5797 C > T mutation compared to those without. Therefore, the presence of c.5797 C > T may partly account for the phenotypic variety of *RP1*-IRD and may yield milder phenotypes. These findings may be useful for predicting the prognosis of *RP1*-IRD patients.

Keywords Retinitis pigmentosa, Cone-rod dystrophy, Macular dystrophy

Retinitis pigmentosa (RP) is a major inherited retinal dystrophy (IRD), affecting approximately 1 in 4000 individuals worldwide[1,2]. In patients with RP, initial symptoms include night blindness and peripheral visual field loss, caused by the degeneration of rod photoreceptors followed by a subsequent loss of visual acuity and central vision due to the degeneration of cone photoreceptors[3].

RP has been reported to be associated with over 80 genes, leading to a variety of genotypes and phenotypes that partly depend on pathogenic mutations. Among the RP-associated genes, *RP1*, *BEST1*, *NR2E3*, *NRL*, *RHO*, and *SAG* are known to be associated with autosomal dominant (AD) RP and autosomal recessive (AR) RP[2,4]. *RP1* consists of four exons that encode a protein of 2,156 amino acids located in the connecting cilia of rod and cone photoreceptors[5,6]. Initially, *RP1* was found to cause AD RP[5,7], and later was reported to be associated with AR RP[8–11]. Subsequently, *RP1* was also associated with cone-rod dystrophy and macular dystrophy (MD)[12,13].

To date, two important and frequent disease-associated variants have been identified. Whole-genome sequencing of Japanese patients with RP revealed a mobile *Alu* element insertion in exon 4 (c.4052_4053ins328 (p.Tyr1352Alafs*9), hereinafter referred to as the *Alu* mutation) as the cause of the disease[14] and was later found to be prevalent among Japanese patients with RP[15]. Many previous studies that screened the *RP1* gene in Japanese RP patients did not report the *Alu* mutation, partly due to the necessity of an optimized screening method to detect this mutation of an extra 328 base pairs[16–18].

Department of Ophthalmology, Nagoya University Graduate School of Medicine, 65 Tsurumai-cho, Showa-ku, Nagoya 466-8560, Japan. ✉email: taro.kominami@gmail.com

Another frequent pathogenic mutation, c.5797 C > T (p.Arg1933*) (hereinafter referred to as the Arg1933* mutation), with a minor allele frequency of 0.6% in the Japanese population, was found to be associated with autosomal recessive macular dystrophy (ARMD)[12] although this may represent a hypomorphic variant, adding complexity to the genotype-phenotype correlation[19]. The high prevalence of specific *RP1* variants, such as the Arg1933* mutation, in the Japanese population may result from a founder effect. This phenomenon, where a small population with limited genetic diversity expands, has been recently reported in other IRD-associated genes and warrants further investigation in this cohort. However, little is known about the phenotype of Arg1933* homozygotes.

Despite previous reports indicating that the Arg1933* mutation drives phenotypic variability in *RP1*-IRD in Japan, the exact role of this mutation in genotype-phenotype correlation remains uncertain. This necessitates a sufficient number of *RP1* patients, with and without the Arg1933* mutation, preferably tested in the same ocular examination setting. Therefore, this study determined the association between genotype and phenotype in patients with *RP1*-IRD from a single center.

Results

Characteristics of the patients

We identified 60 patients with IRD from 55 families carrying pathogenic *RP1* variants. Among these, 42 patients from 39 families had confirmed genetically diagnoses. Table 1 presents the demographic characteristics of these patients. The mean age at the initial visit was 34.8 ± 17.6 years, and 34 patients were followed up for a mean duration of 12.6 ± 8.7 years.

Table 2 shows the genotypes and clinical features of each patient. This study included 12 cases of AD inheritance and 30 cases of AR inheritance. Among the AR cases, 24 had *Alu* mutations, and 14 had Arg1933* mutations. Specifically, there were 8 cases of homozygous *Alu* mutation, 3 cases of homozygous Arg1933* mutation, 8 cases of compound heterozygotes with *Alu* and Arg1933* mutations, and 8 cases with *Alu* mutations combined with other mutations. Genetic analyses for unaffected family members showed that the Alu mutation was detected in a heterozygous state from the mother of NA1039 and NA0039, and from the mother of NA1201 and NA201. Additionally, the c.4196delG/p.Cys1399Leufs*5 variant was detected in a heterozygous state from the mother of NA1209 and NA0209.

Then we categorized the patients into three groups based on inheritance pattern and the presence or absence of the Arg1933* mutation: the AD group, the AR group with the Arg1933* mutation, and the AR group without the Arg1933* mutation. Subsequently, we examined differences in clinical parameters among these three groups. As shown in Fig. 1, the clinical diagnosis was RP in all patients with AD and all AR patients without the Arg1933* mutation. Conversely, AR patients with the Arg1933* mutation showed mostly MD phenotypes with one case of COD and two cases of RP.

Figure 2 shows fundus photographs, fundus autofluorescence images, and horizontal optical coherence tomography (OCT) images of representative cases. The AD group shows peripheral retinal degeneration and abnormal fluorescence in fundus autofluorescence (FAF) images, along with disturbances in the outer retina on OCT. Notably, ellipsoid zone (EZ) lines around the fovea were preserved in both cases (Fig. 2a and b).

Conversely, the AR group without the Arg1933* mutation showed retinal degeneration, which seems to threaten the macula in fundus photographs and FAF images, and severe disturbance in the outer retina on OCT, including the fovea (Fig. 2c and d).

Figure 2e and f present the findings of the AR group with the Arg1933* mutation. Figure 2e depicts a case of ARMD with the Arg1933* mutation, showing retinal degeneration and hypo fluorescence limited to the macula, accompanied by severe outer retinal degeneration in the OCT image. Figure 2f shows a case of AR RP with the Arg1933* mutation, with retinal degeneration across a wide-field of the retina in fundus photographs and FAF images, with outer retinal degeneration while the fovea remains preserved in the OCT image.

Parameters	Data of patients at initial visit ($n = 42$)
Male/female	23/19
Age at initial visit (y.o.)	34.8 ± 17.6 [6, 81]
BCVA at initial visit (logMAR)	0.34 ± 0.51 [−0.11, 2.8]
b-amplitude of ERG (μV)	1830 ± 2212 [0, 8112]
EZ length (μm)	162 ± 166 [5, 568]
HFA 10 − 2 MD value (dB)	−21.4 ± 10.0 [−5.7, −2.2]
	Data of follow-up patients ($n = 34$)
Male/female	19/15
Age at final visit (y.o.)	31.4 ± 15.7 [7, 71]
Follow-up terms (years)	12.6 ± 8.7 [3, 36]
BCVA at final visit (logMAR)	1.02 ± 0.95 [0.00, 2.80]

Table 1. Demographic information of the patients. y.o.: years old, D: Diopter, BCVA: best corrected visual acuity, HFA 10-MD value: mean deviation value of the Humphrey visual field test 10-2 program, EZ: ellipsoid zone, ERG: electroretinogram Data are expressed as mean ± standard deviation [range].

ID (family ID)	Sex	Amino acid change	Phenotype	Age at onset/diagnosis	BCVA	EZ	ERG
		Allele 1/2			RE/LE	RE/LE	RE/LE
N153	M	p.(Leu866fs)/-	AD-RP	38/51	0.80 /0.30	1256/308	12/12
N286	F	p.(Gln678*)/-	AD-RP	49/50	0.22/0.22	1763/2191	49/51
N1006	M	p.(Leu866fs)/-	AD-RP	68/69	0.10/0.10	3053/3008***	27/5.5
N1111	M	p.(Glu729*)/-	AD-RP	39/39	0.05/0.10	3878/3719	87/60
N1125	M	p.(Thr865fs)/-	AD-RP	45/45	0.00/0.00	2785/2510	31/8.5
N1137	F	p.(Leu774*)/-	AD-RP	81/81	0.10/0.00	3303/3080	252/225
N1200	F	p.(Arg677*)/-	AD-RP	Unknown/32	N/A/N/A	N/A/N/A	N/A/N/A
N358	M	p.(Leu866fs)/-	AD-RP	38/42	-0.11/-0.11	1678/1713	154.5/84.5
N597	M	p.(Gln678*)/-	AD-RP	42/42	0.00/0.00	N/A/N/A	N/A/N/A
N741	F	p.(Gln678*)/-	AD-RP	25/39	0.00/0.00	3292/3253	40/51
N809	F	p.(Leu866fs)/-	AD-RP	5/38	0.22/0.22	0/667**	N/A/N/A
N823	F	p.(Gln678*)/-	AD-RP	40/46	0.00/0.00	5957/5942**	128/135
N629	F	m1/m1	AR-RP	11/12	0.22/0.22	553/753**	41/21
N1029	M	m1/m1	AR-RP	7/18	0.70/0.30	0/174**	62/60
N1044	M	m1/m1	AR-RP	11/11	0.10/0.10	N/A/N/A	5/4
NA1039 (family 1)	M	m1/m1	AR-RP	12/26	0.22/0.22	804/0**	N/A/N/A
NA0039 (family 1)	F	m1/m1	AR-RP	6/23	0.10/0.10	246/0**	20/24
NA1048 (family 2)	M	m1/m1	AR-RP	13/13	0.05/0.05	1932/1776**	45/32
NA0048 (family 2)	F	m1/m1	AR-RP	5/12	0.22/0.15	0/0	7/10
NA0070	F	m1/m1	AR-RP	6/25	0.40/0.30	0/0	80/92
NA1201 (family 3)	F	m1/p.(Cys1399fs)	AR-RP	6/7	0.10/0.10	0/943	112/132
NA0201 (family 3)	M	m1/p.(Cys1399fs)	AR-RP	4/15	0.22/0.30	788/435**	20/24
NA1209 (family 4)	F	m1/p.(Cys1399fs)	AR-RP	18/18	0.40/0.15	0/0	28/24
NA0209 (family 4)	M	m1/p.(Cys1399fs)	AR-RP	14/19	0.00/0.00	1924/1460	78 /59
N881	M	m1/p.(Arg396*)	AR-RP	5/7	0.00/0.00	781/534	5/14
N636	M	m1/p.(Gly217fs)	AR-RP	3/14	0.00/0.20	430/0**	19/30
N206	F	m1/p.(Gly217fs)	AR-RP	3/6	0.20/0.40	1413/1826	37/24
N239	F	m1/p.(Ala2498Pro)	AR-RP	29/44	0.05/0.10	N/A/N/A	12/16
N405	M	m1/m2	AR-MD	40/53	1.22/0.30	0/431***	397/311
N442	M	m1/m2	AR-MD	20/26	0.22/0.30	0/0	444/412
N493	M	m1/m2	AR-MD	21/36	1.40/1.40	0/0	327/343
N549	M	m1/m2	AR-MD	29/32	0.22/0.60	282/0**	240/250
N598	F	m1/m2	AR-MD	52/52	0.00 /0.00	4064/4393	220/215
N776	M	m1/m2	AR-MD	42/42	0.10/0.00	993/599	231/260
N838	F	m1/m2	AR-MD	46/46	0.10/0.30	1387/650	281/308
N1122	F	m1/m2	AR-RP	43/44	0.30/0.22	553/810	121/177
nagoya002	M	m2/m2	AR-MD	36/37	0.40/0.15	8112/7598	541/411
N416	M	m2/m2	AR-MD	44/48	0.60/0.70	1357/381	394/389
N437	M	m2/m2	AR-MD	23/23	0.10/0.00	8110/8277	566/566
N1177	M	m2/p.(Gly217fs)	AR-COD	20/33	0.80/1.40	N/A/N/A	N/A/N/A

Continued

ID (family ID)	Sex	Amino acid change Allele 1/2	Phenotype	Age at onset/diagnosis	BCVA RE/LE	EZ RE/LE	ERG RE/LE
N1052	F	m2/p.(Ala1936fs)	AR-MD	41/47	0.22/0.52	653/698	568/548
N1185	F	m2/p.(lle2061fs)	AR-RP	64/64	0.10/0.22	7278/6869	295/177

Table 2. Genotype and the main clinical measures for each RP1-IRD patients. m1: c.4052_4053ins328/p.Tyr1352Alafs*9 (Alu insertion), m2: c.5797 C > T/p.(Arg1933*), RP: retinitis pigmentosa, CACD: central areolar choroidal dystrophy, MD: macular dystrophy, COD: cone dystrophy, RE: right eye, LE: left eye, BCVA: best corrected visual acuity at initial visit (decimal), µm: micro meter, EZ: ellipsoid zone length at initial visit (µm), ERG: flash electroretinogram b-wave amplitude (µV), *: dignosed by referral hospital, **: scanned with cirrus OCT, ***: scanned with RS3000 OCT, M: male, F: female, AD: autosomal dominant, AR: autosomal recessive, N/A: not available

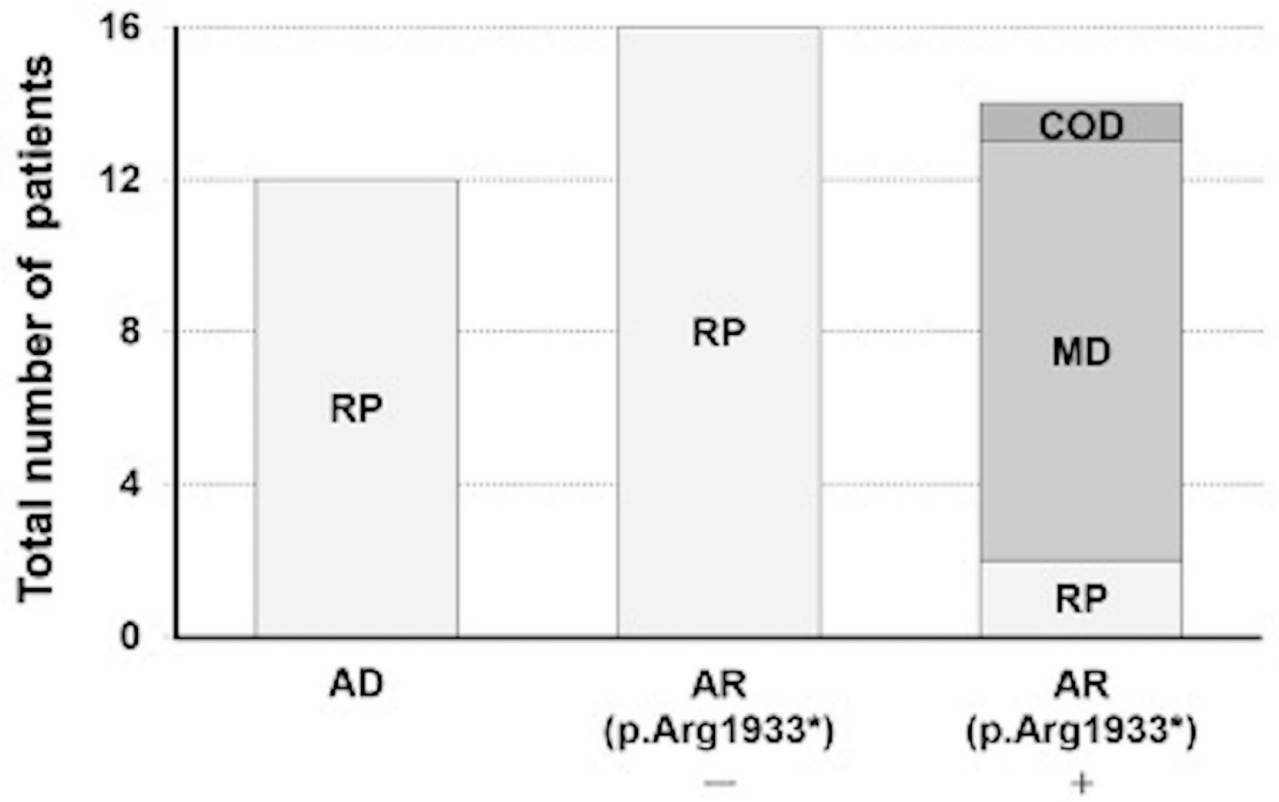

Fig. 1. Clinical diagnosis for each of the three groups. Clinical diagnosis was retinitis pigmentosa (RP) in all autosomal dominant patients (AD) and all autosomal recessive (AR) patients without the Arg1933* mutation (AR (p.Arg1933*−)). Conversely, in AR patients with the Arg1933* mutation (AR (p.Arg1933*+)), clinical diagnosis were mostly macular dystrophy (MD) followed by RP and cone-rod dystrophy (COD).

Significant differences were observed among the groups in terms of age at the initial visit, age at onset, best-corrected visual acuity (BCVA) at the final visit, b-wave amplitude of electroretinogram (ERG), EZ length, and mean deviation value of the Humphrey visual field test 10 − 2 program (HFA 10-2). Figure 3 shows swarm plots for BCVA at the initial visit (Fig. 3a), BCVA at the final visit (Fig. 3b), age at onset (Fig. 3c), EZ length at the initial visit (Fig. 3d), mean deviation value of HFA 10-2 at the initial visit (Fig. 3e), and b-wave amplitudes of the ERG at the initial examination (Fig. 3f).

Regarding BCVA at the initial visit, no significant difference was observed among the three groups (Fig. 3a). However, the BCVA at the final visit for the AR group without the Arg1933* mutation was significantly worse than that for the AD group ($p < 0.05$) (Fig. 3b). The age at onset of the AR group without the Arg1933* mutation was significantly younger than those of the AD and AR with the Arg1933* groups ($p < 0.01$, respectively) (Fig. 3c). Additionally, the EZ length of the AR group without the Arg1933* mutation was significantly shorter than that of the AD group ($p < 0.01$) (Fig. 3d). Furthermore, the mean deviation value of HFA 10 -2 for the AR group without the Arg1933* mutation was significantly worse compared to the AD and AR with the Arg1933* groups ($p < 0.05$, respectively) (Fig. 3e). Lastly, the ERG b-wave amplitudes of the AR group with the Arg1933* mutation were significantly larger than those of the AD and AR without the Arg1933* groups ($p < 0.01$, respectively) (Fig. 3f).

Longitudinal analyses of visual parameters between three groups

Figure 4a shows longitudinal plots of BCVA, and Fig. 4b illustrates the EZ length. The AD group is represented by black plots, the AR group without the Arg1933* mutation by red plots, and the AR group with the Arg1933* mutation by blue plots.

Regarding both BCVA and EZ length, the AR group without the Arg1933* mutation was monitored from the teenage years to the 40s due to its relatively early onset, the AR group with the Arg1933* mutation from around the 20–40 s to the 60s, and the AD group from around the 50s to the 80s due to its relatively late onset. Across all three groups, some cases had acute periods of BCVA loss. However, in most cases within all three groups, the EZ lengths tended to remain relatively stable over a long period. The coefficients obtained from linear regression analyses showed no significant differences between the three groups in terms of BCVA and EZ length.

Multiple regression analysis

Generalized linear mixed-effects regression models with backward stepwise model selection using Akaike information criterion (AIC) showed that the explanatory variables of b-wave amplitudes of ERG ($p < 0.001$),

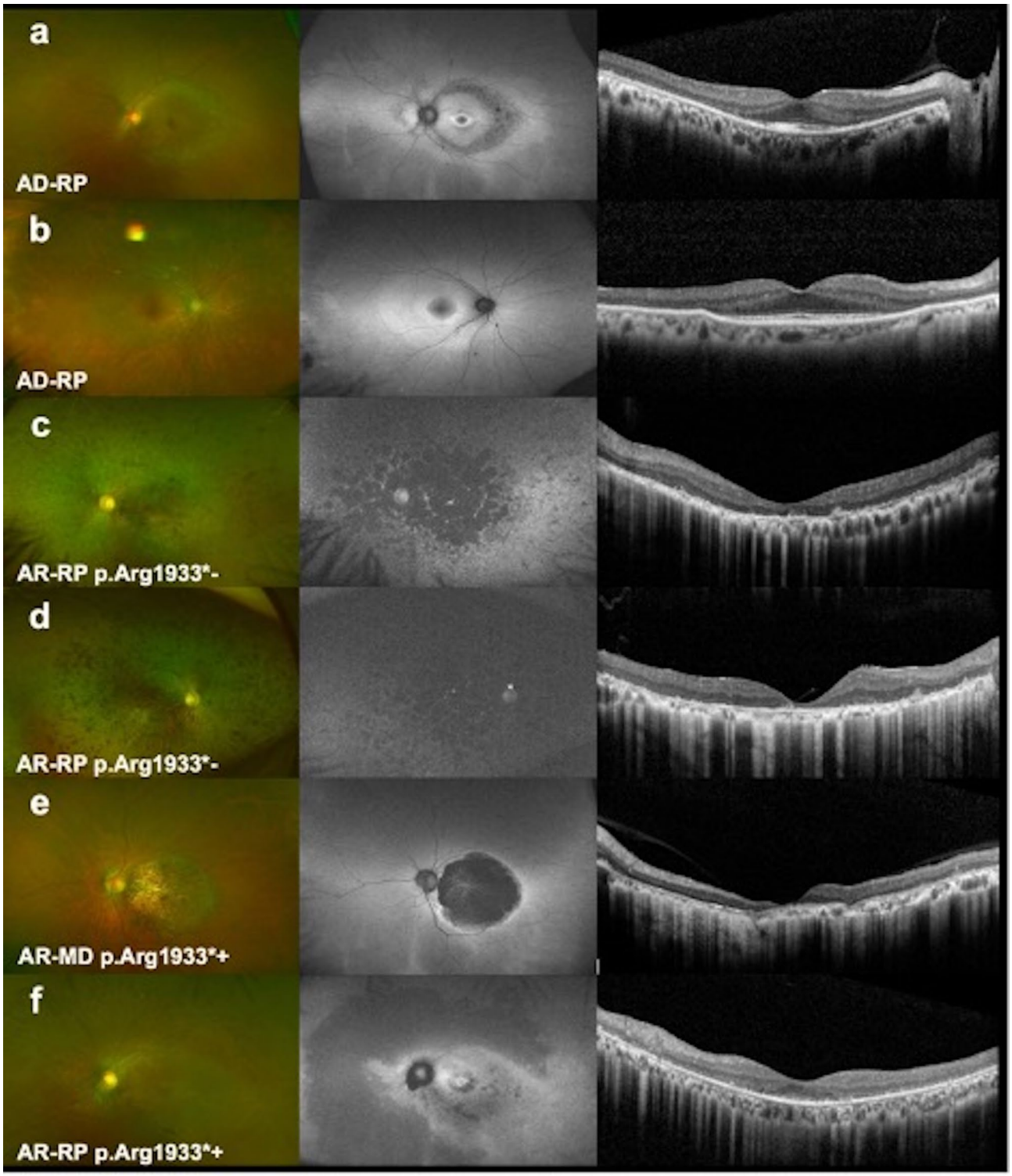

Fig. 2. Fundus color photographs, fundus autofluorescence images, and horizontal optical coherence tomography images of representative cases. Each panel shows fundus color photographs (left), fundus autofluorescence images (middle), and horizontal optical coherence tomography images (right) obtained from the same patient. Multimodal retinal imaging of the left eye of a 50-year-old male patient (N358) with AD-RP carrying a heterozygous p.(Leu866fs) mutation (**a**); the right eye of an 83-year-old female patient (N1137) with AD-RP carrying a heterozygous p. (Leu774*) mutation (**b**); the left eye of a 40-year-old female patient (N1201) with AR RP carrying compound heterozygous mutations of p. Tyr1352Alafs*9/p. (Cys1399fs) (**c**); the right eye of a 37-year-old male patient with AR RP carrying compound heterozygous mutations of p. Tyr1352Alafs*9/p. (Cys1399fs) (**d**); the left eye of a 64-year-old male patient with AR RP carrying compound heterozygous mutations of p. Tyr1352Alafs*9/ (p. Arg1933* -) (**e**); and the left eye of a 47-year-old female patient with AR RP carrying compound heterozygous mutations of p. Tyr1352Alafs*9 (p. Arg1933*-) (**f**).

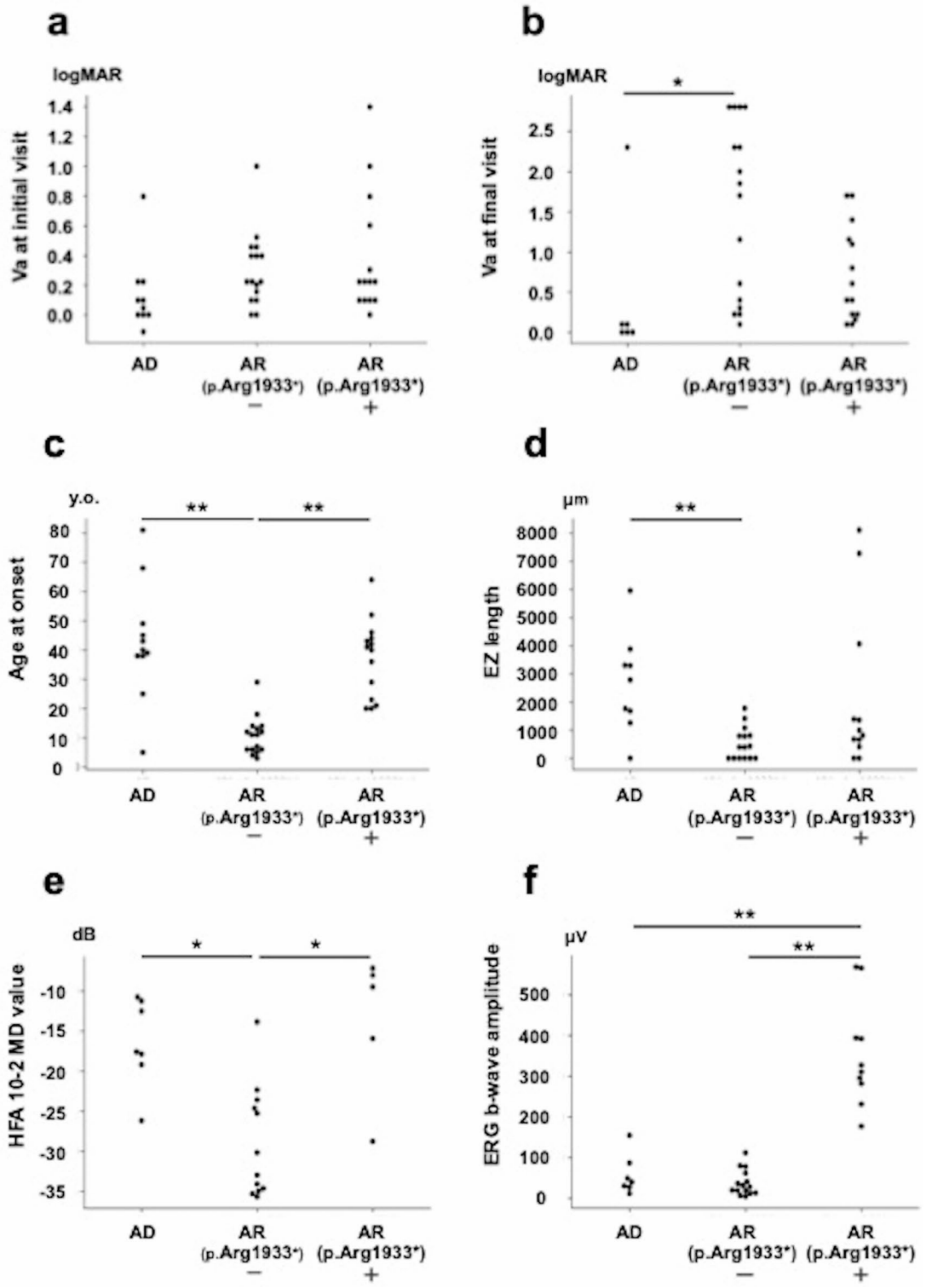

Fig. 3. Comparison of visual parameters and patient information between three groups. These figures show swarm plots of best-corrected visual acuity (BCVA) at the initial visit (**a**), BCVA at the final visit (**b**), age at onset (**c**), ellipsoid zone (EZ) length at the initial visit (**d**), mean deviation (MD) value of the Humphrey visual field test 10-2 program at the initial visit (**e**), and electroretinogram (ERG) b-wave amplitudes at the first examination (**f**) of the autosomal dominant (AD) group, autosomal recessive cases without the Arg1933* (AR p.Arg1933*−) group, and autosomal recessive cases without the Arg1933* (AR p.Arg1933*+) group. * $P < 0.05$, ** $P < 0.01$ using the Steel-Dwass test.

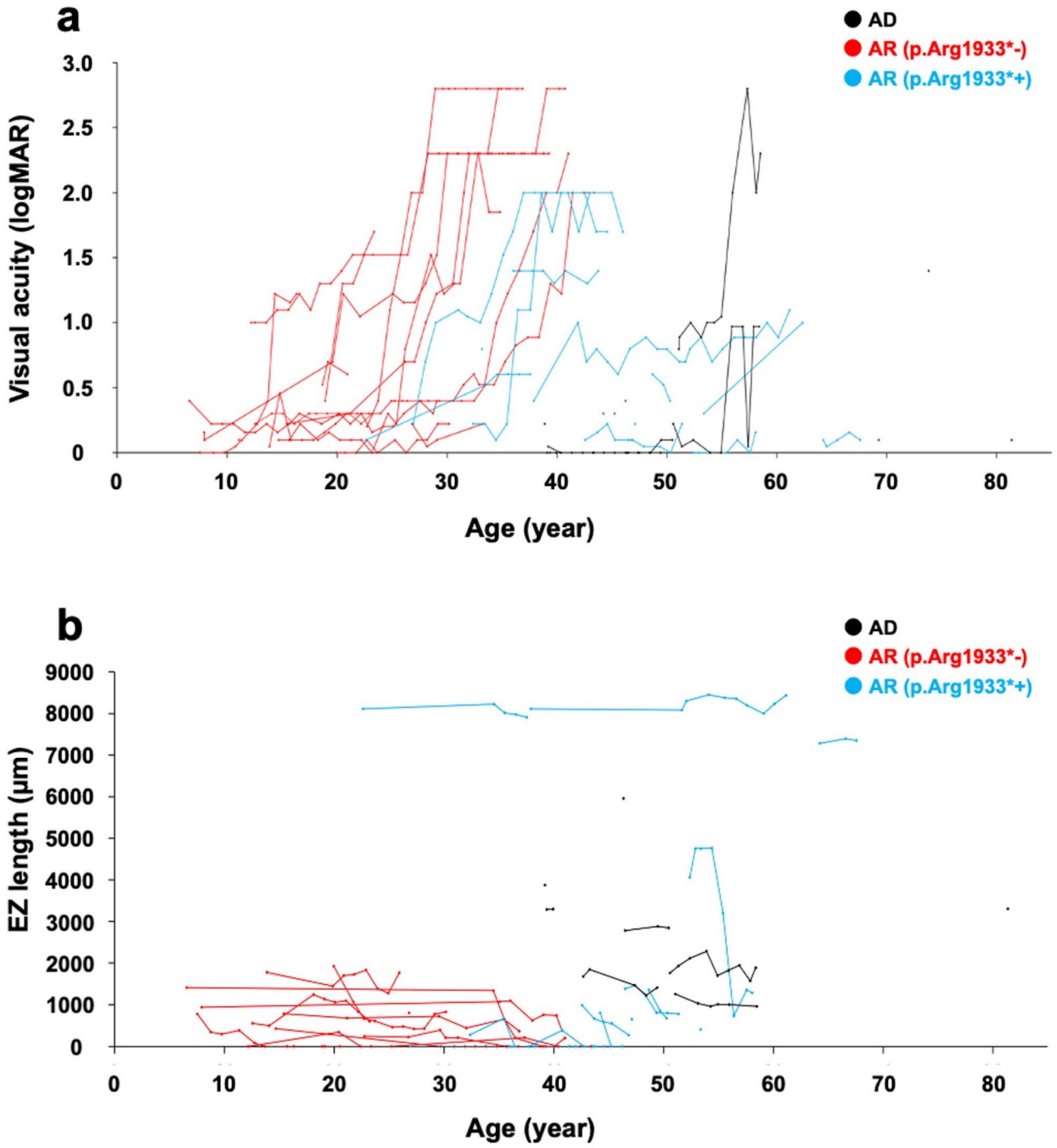

Fig. 4. Comparison of the long-term course of visual function between the three groups. Longitudinal plots of best-corrected visual acuity (BCVA) (**a**) and ellipsoid zone (EZ) length (**b**) are shown. The black plot represents autosomal dominant (AD), the red plot represents autosomal recessive cases without the Arg1933* (AR p.Arg1933*−) and blue plot shows autosomal recessive cases with the Arg1933* (AR p.Arg1933*+).

age at the initial visit ($p < 0.01$), and EZ length at the initial visit ($p = 0.017$) were the most effective variables to distinguish between the AD group, the AR group without the Arg1933* mutation, and the AR group with Arg1933* mutation (Table 3).

Discussion

This study assessed the association between the phenotype and *RP1* variants in patients with IRD and showed that the phenotype of *RP1*-related AR-IRD has different characteristics depending on the presence of a common nonsense mutation close to the C-terminus, c.5797 C > T (p.Arg1933*).

	Standardized partial Regression coefficient (β)	95% CI [0.025, 0.975]	*p*-value	VIF
b-wave amplitude of ERG (μV)	2.2	1.8, 2.7	6.23×10^{-15}	1.17
age at first visit (yrs)	−0.88	−1.40, −0.36	0.0015	1.2
EZ length at first visit (μm)	−0.59	−1.06, −0.12	0.017	1.21

Table 3. Multivariate generalized linear mixed effects model between groups and explanatory variables. ERG: electroretinogram, EZ: ellipsoid zone, CI: confidence interval, VIF: variance inflation factor.

Previous studies[1,2] reported that variants in the *RP1* gene are associated with a wide range of progressive retinal dystrophies, and that ARMD and AR COD often involve hypomorphic gene mutations, including the Arg1933* mutation. Consistent with these findings, our study also revealed a high proportion of macular and cone dystrophies among patients with the Arg1933* mutation.

A previous study has reported that individual homozygotes for the Arg1933* mutation maintain a normal phenotype even at 80 years of age[19]. However, in this study, three individuals with homozygosity for the Arg1933* mutation showed MD. This suggests that homozygosity for the Arg1933* mutation may also contribute to the onset of IRD.

The observed milder phenotype in patients with the Arg1933* mutation can be partly explained by the location of the mutation within the *RP1* gene. This nonsense mutation occurs near the C-terminus of *RP1*, leaving two critical functional domains intact: the Drosophila melanogaster bifocal (BIF) domain (amino acids 486–635)[5], which is needed for normal photoreceptor morphogenesis, and the doublecortin (DCX) domain (amino acids residues 36 to 118 and 154 to 233)[5,7], which involves with microtubules. The preservation of these domains may allow for partial retention of *RP1* function, accounting for the milder phenotypes, such as macular dystrophy, observed in patients carrying this variant. Moreover, the Arg1933* mutation is downstream of the region associated with AD-RP. Studies have shown that truncating mutations located between p.500 and p.1053 often exert a dominant-negative effect or result in a gain of function, contributing to the more severe phenotypes characteristic of AD-RP. In contrast, mutations located between p.1053 and p.1815 are typically associated with AR inheritance, likely due to loss-of-function effects. This suggests that truncating mutations, such as Arg1933*, in the last 340 nucleotides of *RP1* might be less pathogenic or act as hypomorphic variants, leading to the milder phenotypes observed in patients with autosomal recessive *RP1*-IRD. This aligns with previous findings where non-pathogenic truncating mutations were identified in the C-terminal region of *RP1*.

The phenotype of patients without the Arg1933* mutation was predominantly RP in almost all cases. In contrast, patients with the Arg1933* mutation showed COD, MD, and RP. Therefore, the presence of the Arg1933* mutation may contribute to the phenotypic variability observed in *RP1*-IRD. This finding aligns with previous studies that have identified compound heterozygous variants, including hypomorphic variants, with a pathogenic variant reported in patients with AR-RP[10,12,20,21].

However, there is also a possibility that phenotypic variability depends on other factors, such as interactions with additional genes, including *EYS*, which has been implicated in ciliary axonemes as well as *RP1*[22]. This study did not detect other pathogenic *RP1* mutations and mutations in other genes although further studies may explore the role of additional variants in modifying the *RP1*-related phenotypes.

We previously demonstrated that the founder *Alu* insertion in the *RP1* gene is a significant cause of AR RP in a Japanese cohort[15]. Another multicenter study in Japan reported that the *Alu* mutation is the most common variant in Japanese patients with *RP1*-IRD[23]. The *Alu* mutation was detected in many cases of AR-IRD in this study. Therefore, the *Alu* mutation may also play an important role in determining the phenotype of *RP1*-IRD, similar to the Arg1933* mutation.

This study evaluated various visual parameters to compare the severity of *RP1*-related IRD in patients based on their inheritance pattern or genetic characteristics. In terms of comparing the inheritance patterns of *RP1*-related RP between AD and AR, the visual acuity at the final visit of the AR group without the Arg1933* mutation was significantly worse than that of the AD group, although there was no significant difference in visual acuity at the initial visit between the AD group and the AR group without the Arg1933* mutation. Therefore, AD RP progresses more slowly than AR RP without the Arg1933* mutation. This finding is consistent with well-known reports that AR RP tends to be more severe than AD RP, as previously described[23,24].

In this study, the age at onset of the AR group without the Arg1933* mutation was significantly younger than that of both the AR group with the Arg1933* mutation and the AD group. This finding suggests that the AR group without the Arg1933* mutation may be a more severe phenotype compared to the AR group with the Arg1933* mutation, despite having the same inheritance pattern. The HFA mean deviation value also demonstrated similar results to the age at onset. These findings indicate that the presence of the Arg1933* mutation influences the severity of *RP1*-IRD and its associated phenotype.

The AR group with the Arg1933* mutation showed a significantly reduced ERG response compared to both the AD group and the AR group without the Arg1933* mutation. This result does not necessarily indicate a severity difference between these groups but rather reflects a phenotype difference between RP (seen in the AD group and the AR group without the Arg1933* mutation) and MD (seen in the AR with the Arg1933* mutation).

The EZ lengths of the AR group without the Arg1933* mutation were significantly shorter than those of the AD group. This finding may support the hypothesis that the AR RP without the Arg1933* mutation is more severe than AD RP.

In contrast, there were no statistically significant differences in EZ lengths between the AR group without the Arg1933* mutation and the AR group with the Arg1933* mutation. This finding reflects the fact that the phenotype of the AR group with the Arg1933* mutation mainly showed MD, which often involves impaired outer retinal structures in the macular region.

In this study, we performed subgroup analyses of the AD, AR without the Arg1933* and AR with the Arg1933* mutation groups based on phenotype and genomic information. This grouping approach is consistent with that used in a previous study[23]. We hypothesized that certain parameters determine the differences among these groups.

Multiple regression analysis revealed that the combination of b-wave amplitude of ERG, age at the initial visit, and EZ length was the most effective factor combination for explaining the grouping of these three groups. ERG amplitudes seem to be important for distinguishing the groups with or without the Arg1933* mutation, which mainly reflects the classification of RP or MD. Age at the initial visit and EZ length may contribute to differences in severity between the AD and AR groups without the Arg1933* mutations, both of which included patients with RP. These two parameters might be important for categorizing RP patients into AD RP or AR RP groups based on severity. Notably, it was not a single parameter but rather a combination of these factors that appeared to determine these groupings, which are correlated with severity and phenotype.

Moreover, this study performed a longitudinal analysis of BCVA and EZ length, observing the characteristic progression rate of AR cases in the Arg1933* mutation group. Unlike the previous reports[23,25], we categorized the cases based on the presence or absence of the Arg1933* mutation. The rate of BCVA loss was most rapid in the AR group without the Arg1933* mutation, followed by the AR group with the Arg1933* mutation, and finally the AD group.

Since the AR group without the Arg1933* mutation has been considered the most severe based on previous analyses using visual function parameters, it is reasonable that visual acuity decline occurs earliest in this group. This finding aligns with a previous study that observed rapid progression in the AR group without the Arg1933* mutation[23]. The AR group with Arg1933* mutation progressed faster than the AD group. This may be attributed to the fact that many patients in this group presented with an MD phenotype, which likely caused central visual function loss.

We performed a linear regression analysis to assess the rate of exacerbation in these three groups after onset; however, we observed no significant difference among the progression rates of these groups. Although the onset differed among the three groups, they commonly had a rapid deterioration in BCVA, which may explain why there were no differences in the rate of progression. Once central retinal function, upon which BCVA depends, begins to deteriorate, it may rapidly decline within a few years across all three groups.

The AR group without the Arg1933* mutation tended to have shorter EZ lengths than the AD group. In the AR group with the Arg1933* mutation, where most phenotypes are characterized by MD, there was substantial variation from case to case, and EZ length did not change significantly over 20 years, even in cases where the EZ was relatively well preserved. Therefore, factors other than *RP1* may be involved in this condition.

This study has several limitations. First, being a single-center study introduces the possibility of regional biases, although it has a strength in terms of comparing clinical findings. Second, this study has missing values due to its retrospective nature. Third, segregation studies have not been performed on all cases, therefore true compound heterozygosity or homozygosity has not been confirmed in all cases. More accurate prognostic information may be provided by future prospective studies. Furthermore, the phenotype of IRD may change over time; therefore, the phenotypes analyzed in this study may change in the future.

In conclusion, this study demonstrated an association between phenotype and pathogenic mutations in *RP1*-IRD patients. It appears that the presence of the c.5797 C > T mutation may contribute to the phenotypic variability of *RP1*-IRD and may lead to milder phenotypes in AR *RP1*-IRD. These findings could be valuable for predicting the prognosis of *RP1*-IRD patients and may also aid in the development of personalized medicine, such as gene therapy, in the future.

Methods

Participants

In this retrospective observational study, we reviewed the medical charts of patients who visited the ophthalmology department at Nagoya University Hospital and were diagnosed with inherited retinal dystrophy. Written informed consent was obtained from all patients. The protocol of this study followed the principles outlined in the Declaration of Helsinki and was approved by the Institutional Review Board/Ethics Committee of Nagoya University Hospital(approval number: 2020-0598).

All patients underwent ophthalmic examinations, including measurement of BCVA, assessment of refractive errors, biomicroscopy using a slit-lamp microscope, fundus examinations, OCT, FAF imaging, HFA 10-2 and ERG.

Clinical diagnosis

All patients were diagnosed with IRD by physicians specializing in IRD. The diagnosis of RP included symptoms such as night blindness, photophobia, tunnel vision, visual acuity loss, bone spicule pigmentation, characteristic findings on fundus examination (e.g., vessel attenuation, abnormal fluorescence on FAF), disruption of the retinal outer layers seen on OCT (e.g., blurred or shortened ellipsoid zone), and reduced responses on full-field ERGs. Atypical RP cases, such as segmental RP or nonpigmented RP, were included in this study if they had typical RP abnormalities, including vessel attenuation, disruption of retinal outer layers, and reduced ERG responses. COD was diagnosed based on symptoms such as visual acuity loss or photophobia, retinal degeneration observed on fundus examination, disruption of the retinal outer layers seen on OCT, or reduced cone responses on full-

field ERGs with normal rod responses. MD was diagnosed in patients who had symptoms or abnormalities on fundus examination and OCT similar to COD but with normal full-field ERG responses or reduced cone and rod responses on focal macular ERGs or multifocal ERGs.

Genetic analyses

Genomic DNA was extracted from blood or saliva samples obtained from patients and some of the unaffected family members, and analyzed by targeted resequencing for 86 genes using a next-generation sequencer, following the methodology described in previous reports[26]. Pathogenic variants were determined according to the J-IRD-VI guidelines[27]. We selected patients who had *RP1* gene variants classified as pathogenic or likely pathogenic. As described in previous studies[15,28], we conducted a search for *Alu* sequences in FASTQ files generated by the next-generation sequencing using a grep search program[29]. After screening of this program, we performed polymerase chain reaction and electrophoresis to detect the *Alu* mutation which has been suggested to be associated with autosomal recessive RP, as previously reported[15], as *Alu* mutations cannot be detected using next-generation sequencing alone. Patients with homozygous or compound heterozygous variants that were classified as pathogenic, or those with heterozygous variants affecting amino acid residue numbers 677 to 917, which have been previously reported as autosomal dominant[30], were considered as resolved cases. Some cases were included in the previously reported analyses[19] (NA0039, NA1039, NA0048, NA1048, NA0070, NA0201, NA1201, NA0209, and NA1209).

Clinical evaluations

We assessed clinical features such as sex, family history, age at onset, age at the initial visit, BCVA, length of EZ on OCT images, mean deviation value of HFA 10 -2 program, and ERG amplitudes. These parameters were compared among three groups: AD, AR without the Arg1933* mutation and AR with the Arg1933* mutation. Decimal BCVA was converted to logarithm of the minimum angle of resolution (logMAR) units for statistical analyses. LogMAR values for counting fingers, hand motion, light perception, and no light perception were assigned as 1.85, 2.30, 2.80, and 2.90, respectively, as reported previously[31]. OCT images were obtained using spectral domain OCT devices, such as Spectralis OCT (Heidelberg Engineering, Heidelberg, Germany), RS-3000 (NIDEK, Gamagori, Japan) or Cirrus (Carl Zeiss, Oberkochen, Germany). The length of the EZ extending from the fovea was manually measured on horizontal OCT images using the built-in calipers of OCT devices. We defined the border of the EZ as the location where the EZ band met the upper surface of the RPE for ease of identification, as reported previously[32]. Data from the right eye of each case were analyzed, except in cases of amblyopia (two cases), vitrectomized eye (one case), and macular hole (one case), where data from the left eye were analyzed, except for multivariable regression analysis. Visual acuity and EZ length were longitudinally evaluated using data from all past visits to Nagoya University Hospital. For longitudinal analyses, linear regression analyses were performed for each case, and the obtained coefficients were evaluated.

For further multivariable regression analyses with the three groups as categorical response variables and age at onset, age at the initial visit, BCVA, EZ length on OCT images, and b-wave amplitude as the explanatory variables, we conducted generalized linear mixed-effects regression analyses with a random intercept. This approach was chosen due to the high correlation of the response variables between right and left eyes. We constructed a multivariable model using backward stepwise selection with AIC to determine the best predictive model by selecting the most relevant explanatory variables. Standardized partial regression coefficients (β) were then calculated for the independent variables after standardizing all variables to a mean of 0 and variance of 1. We also calculated the variance inflation factor to assess the severity of multicollinearity.

We used Fisher's exact test to compare categorical variables. Moreover, one-way ANOVA was performed to compare parametric continuous variables, whereas the Kruskal–Wallis test was used to compare nonparametric continuous variables. The Steel–Dwass tests were used to determine the significance of differences between various parameters obtained above for multiple comparison tests. A p-value less than 0.05 was considered statistically significant. These analyses were performed using scikit-learn version 0.24.0 based on Python version 3.6.7 and R version 4.4.2.

Data availability

Data are available in a public, open access repository. We have uploaded the variants reported in this study to ClinVar, which can be accessed at the following link: https://www.ncbi.nlm.nih.gov/clinvar/submitters/509444.

Received: 7 August 2024; Accepted: 22 October 2024
Published online: 27 October 2024

References

1. Pagon, R. A. Retinitis pigmentosa. *Surv. Ophthalmol.* **33**, 137–177 (1988).
2. Verbakel, S. K. et al. Non-syndromic retinitis pigmentosa. *Prog. Retin. Eye Res.* **66**, 157–186 (2018).
3. Hartong, D. T., Berson, E. L. & Dryja, T. P. Retinitis pigmentosa. *Lancet* **368**, 1795–1809 (2006).
4. Ran, X. et al. 'RetinoGenetics': A comprehensive mutation database for genes related to inherited retinal degeneration. *Database (Oxford)* **2014**, bau047 (2014).
5. Pierce, E. A. et al. Mutations in a gene encoding a new oxygen-regulated photoreceptor protein cause dominant retinitis pigmentosa. *Nat. Genet.* **22**, 248–254 (1999).
6. Liu, Q. et al. Identification and subcellular localization of the RP1 protein in human and mouse photoreceptors. *Invest. Ophthalmol. Vis. Sci.* **43**, 22–32 (2002).
7. Sullivan, L. S. et al. Mutations in a novel retina-specific gene cause autosomal dominant retinitis pigmentosa. *Nat. Genet.* **22**, 255–259 (1999).

8. Khaliq, S. et al. Novel association of RP1 gene mutations with autosomal recessive retinitis pigmentosa. *J. Med. Genet.* **42**, 436–438 (2005).
9. Ferré, C., Espino, A., Cruzado, J. M. & Carratalá, J. Severe neurologic toxicity from oral acyclovir. *Med. Clin. (Barc).* **98**, 679 (1992).
10. Avila-Fernandez, A. et al. Identification of an RP1 prevalent founder mutation and related phenotype in Spanish patients with early-onset autosomal recessive retinitis. *Ophthalmology*. **119**, 2616–2621 (2012).
11. Kurata, K., Hosono, K. & Hotta, Y. Clinical and genetic findings of a Japanese patient with RP1-related autosomal recessive retinitis pigmentosa. *Doc. Ophthalmol.* **137**, 47–56 (2018).
12. Verbakel, S. K. et al. Macular dystrophy and cone-rod dystrophy caused by mutations in the RP1 gene: extending the rp1 disease spectrum. *Invest. Ophthalmol. Vis. Sci.* **60**, 1192–1203 (2019).
13. Riera, M. et al. Expanding the retinal phenotype of RP1: from retinitis pigmentosa to a novel and singular macular dystrophy. *Br. J. Ophthalmol.* **104**, 173–181 (2020).
14. Nishiguchi, K. M. et al. Whole genome sequencing in patients with retinitis pigmentosa reveals pathogenic DNA structural changes and NEK2 as a new disease gene. *Proc. Natl. Acad. Sci. USA*. **110**, 16139–16144 (2013).
15. Nishiguchi, K. M. et al. A founder Alu insertion in RP1 gene in Japanese patients with retinitis pigmentosa. *Jpn J. Ophthalmol.* **64**, 346–350 (2020).
16. Oishi, M. et al. Comprehensive molecular diagnosis of a large cohort of Japanese retinitis pigmentosa and Usher syndrome patients by next-generation sequencing. *Invest. Ophthalmol. Vis. Sci.* **55**, 7369–7375 (2014).
17. Maeda, A. et al. Development of a molecular diagnostic test for retinitis pigmentosa in the Japanese population. *Jpn J. Ophthalmol.* **62**, 451–457 (2018).
18. Kawamura, M. et al. Novel 2336-2337delCT mutation in RP1 gene in a Japanese family with autosomal dominant retinitis pigmentosa. *Am. J. Ophthalmol.* **137**, 1137–1139 (2004).
19. Nikopoulos, K. et al. A frequent variant in the Japanese population determines quasi-mendelian inheritance of rare retinal ciliopathy. *Nat. Commun.* **10**, 2884 (2019).
20. Wang, P. et al. An ophthalmic targeted exome sequencing panel as a powerful tool to identify causative mutations in patients suspected of hereditary eye diseases. *Transl Vis. Sci. Technol.* **8**, 21 (2019).
21. Neveling, K. et al. Next-generation genetic testing for retinitis pigmentosa. *Hum. Mutat.* **33**, 963–972 (2012).
22. Alfano, G. et al. EYS is a protein associated with the ciliary axoneme in rods and cones. *PLoS One*. **11**, e0166397 (2016).
23. Mizobuchi, K. et al. Genotype-phenotype correlations in RP1-associated retinal dystrophies: a multi-center cohort study in Japan. *J. Clin. Med.* **10**, 2265 (2021).
24. Lafont, E. et al. Patients with retinitis pigmentosa due to RP1 mutations show greater severity in recessive than in dominant cases. *J. Clin. Exp. Ophthalmol.* **2**, 12 (2012).
25. Ueno, S. et al. Clinical characteristics and high resolution retinal imaging of retinitis pigmentosa caused by RP1 gene variants. *Jpn J. Ophthalmol.* **64**, 485–496 (2020).
26. Koyanagi, Y. et al. Genetic characteristics of retinitis pigmentosa in 1204 Japanese patients. *J. Med. Genet.* **56**, 662–670 (2019).
27. Fujinami, K., Nishiguchi, K. M., Oishi, A., Akiyama, M. & Ikeda, Y. Specification of variant interpretation guidelines for inherited retinal dystrophy in Japan. *Jpn J. Ophthalmol.* **68**, 389–399 (2024).
28. Goto, K. et al. Disease-specific variant interpretation highlighted the genetic findings in 2325 Japanese patients with retinitis pigmentosa and allied diseases. *J. Med. Genet.* **61**, 613–620 (2023).
29. Won, D. et al. In silico identification of a common mobile element insertion in exon 4 of RP1. *Sci. Rep.* **11**, 13381 (2021).
30. Nanda, A., McClements, M. E., Clouston, P., Shanks, M. E. & MacLaren, R. E. The location of exon 4 mutations in RP1 raises challenges for genetic counseling and gene therapy. *Am. J. Ophthalmol.* **202**, 23–29 (2019).
31. Grover, S., Fishman, G. A., Alexander, K. R., Anderson, R. J. & Derlacki, D. J. Visual acuity impairment in patients with retinitis pigmentosa. *Ophthalmology*. **103**, 1593–1600 (1996).
32. Kominami, T. et al. Associations between outer retinal structures and focal macular electroretinograms in patients with retinitis pigmentosa. *Invest. Ophthalmol. Vis. Sci.* **58**, 5122–5128 (2017).

Acknowledgements

This work was supported by the Japan Society for the Promotion of Science (JSPS) KAKENHI (23K15929 to TK and 23H03059 to KMN) and grants from Japan Agency for Medical Research and Development (23ym0126071h0002 and 23ek0109660h0001 to KMN), The manuscript was edited by a professional English editing service (Enago).

Author contributions

KN analysed data and drafted the manuscript. TK acquired data, analysed data, drafted the manuscript and obtained funding. KG, YK, JO, KK, KYa, OT and KYu acquired data and analysed data. TI contributed to statistical analysis and drafted the manuscript. KMN provided conception, drafted the manuscript and obtained funding. HU provided conception, drafted the manuscript. All authors contributed to study conception and design, and approved the final version of manuscript.

Declarations

Competing interests

The authors declare no competing interests.

Additional information

Supplementary Information The online version contains supplementary material available at https://doi.org/10.1038/s41598-024-77441-3.

Correspondence and requests for materials should be addressed to T.K.